Mass-fractal clustering and power-law decay of cluster size in 1-propanol aqueous solution

M. Misawa,[a] I. Dairoku, A. Honma, Y. Yamada, T. Sato, and K. Maruyama
Department of Chemistry, Faculty of Science, Niigata University, Niigata 950-2181, Japan

K. Mori,[b] S. Suzuki, and T. Otomo
Neutron Science Laboratory, Institute of Materials Structure Science, KEK, Tsukuba 305-0801, Japan

(Received 8 March 2004; accepted 16 June 2004)

Mesoscale structure of 1-propanol aqueous solutions with propanol mole fraction x_p ranging from 0.1 to 0.33 has been studied by means of small angle neutron scattering (SANS) and large-scale reverse Monte Carlo (RMC) technique. Analysis of the SANS intensities in terms of a fractal model shows that the fractal dimension d_f of mesoscale structure of the solution is about 1.8–1.9 for water-rich solution and about 1.5 for propanol-rich solution. Percolation analysis on the RMC results reveals that the water molecules and the propanol molecules cluster, respectively, as a mass fractal, the dimension d_M of which is about 2.3–2.5 for both clusters for water-rich solution. Furthermore, the distribution of the cluster size is expressed by a simple power law with an exponent τ of about 1.35–1.5 for the propanol clusters and 1.05–1.2 for the water clusters. These results imply that the current solution is characterized by polydisperse mass fractals. In fact, a theoretical relation for polydisperse system of mass fractals, $d_f = d_M(2-\tau)$, holds well in the current solution. The characteristic change in d_f from 1.8–1.9 to 1.5 described above is attributed to the crossover between the water-rich regime and the propanol-rich regime. Most of the water molecules and the propanol molecules are located on the interface between clusters, and the water molecules form thin layers of about 10 Å thick irrespective of 1-propanol content studied. © *2004 American Institute of Physics.* [DOI: 10.1063/1.1780931]

I. INTRODUCTION

Water plays an important role in various fields of natural science. One of the most interesting issues relating to water may be its role in assisting self-organization of macromolecules such as proteins. However the biological system is so complicated that the role of water in such system is still obscure. Detailed information on the physical and chemical properties of water in much simpler solutions is helpful to understand the role of water in more complicated systems. The reentrant phase-separation phenomenon[1,2] observed in some aqueous solutions of small molecules such as alcohol is one of the simple examples of self-organization of a solute in aqueous solution. However, the role of water has not been clarified even in such a simple solution.

We have studied the reentrant phase-separation phenomena of 1-propanol aqueous solution[2] by means of small angle neutron scattering (SANS) and a large-scale reverse Monte Carlo (RMC) analysis in order to clarify the role of water in this system.[3,4] We have studied the solution of only one composition of 1-propanol with 0.167 mole fraction. It was found[3] that the mesoscale structure of the solution was characterized by a fractal with a fractal dimension d_f of about 1.9. Furthermore it was found that the solvent water formed thin layers of about 10 Å thick or less in the solution.[4] However, the role of water in the phase separation of the current solution has not been clear. This paper reports more details on the mesoscale structure of the current solution especially on its composition dependence.

II. EXPERIMENT AND DATA ANALYSIS

A. Small angle neutron scattering

The samples measured here were the solutions of 1-propanol (C_3H_7OH) and heavy water (D_2O). The use of heavy water was just to increase the neutron contrast between the two molecules. The compositions of 1-propanol x_p of the solutions ranged from 0.1 to 0.33 in mole fraction. The values of x_p are listed in Table I. A small amount of salt, KCl, was added to each solution in order to enhance the concentration fluctuation. We have already confirmed that the addition of salt does not affect the fractal dimensionality of the solution.[3] The composition of KCl x'_{KCl} for each solution is listed in Table I. Because the phase separation temperature depends on the concentration of salt,[2] the values of x'_{KCl} listed in Table I were so controlled that every solution has the similar phase-separation temperature or the similar thermodynamic state at room temperature, except for the solution of $x_p = 0.33$ on which we did not observe any clear sign for the phase separation. SANS experiments were carried out at 25 °C using the small/wide-angle neutron diffractometer (SWAN)[5] at the KENS pulsed neutron source of High Energy Accelerator Research Organization KEK, Japan. The scattering intensity was corrected for the

[a]Author to whom correspondence should be addressed. Electronic mail: misawa@chem.sc.niigata-u.ac.jp
[b]Present address: Research Reactor Institute, Kyoto University, Osaka 590-2181, Japan.

TABLE I. Concentration of 1-propanol aqueous solution studied by small angle neutron scattering. x_p is mole fraction of 1-propanol and $x_w(=1-x_p)$ is that of water. Both values are defined for salt-free solution. x'_{KCl} is mole fraction of KCl added to solution. Mole fraction of 1-propanol x'_p and that of water x'_w for salt-added solution are given by $x'_p=x_p(1-x'_{\mathrm{KCl}})$ and $x'_w=x_w(1-x'_{\mathrm{KCl}})$, respectively.

x_p	x_w	x'_{KCl}
0.10	0.90	0.0249
0.125	0.875	0.0234
0.167	0.833	0.0208
0.19	0.81	0.0195
0.22	0.78	0.0177
0.25	0.75	0.0159
0.29	0.71	0.0134
0.33	0.67	0.0110

incoherent-inelastic scattering[6] from H atoms in addition to the standard corrections for transmission and cell scattering.

B. Data analysis by fractal model

The SANS intensity $I(Q)$ was analyzed in terms of a fractal model.[7,8] As the details of the analysis procedure have been given in a previous paper,[3] a brief explanation is given here. The $I(Q)$ is given by

$$I(Q)=\alpha[I_{\mathrm{fr}}(Q)+I_{\mathrm{self}}(Q)], \tag{1}$$

where Q is a scattering vector defined as $Q=4\pi\sin\theta/\lambda$ with a scattering angle 2θ and a neutron wavelength λ, α a proportional constant, $I_{\mathrm{fr}}(Q)$ a structure factor for fractal object, and $I_{\mathrm{self}}(Q)$ a self term. The $I_{\mathrm{fr}}(Q)$ and $I_{\mathrm{self}}(Q)$ are given by Eqs. (2) (Refs. 3 and 8) and (3), respectively,

$$I_{\mathrm{fr}}(Q)=x_p^2x_w^2[\langle f_u(Q)\rangle\delta-\Delta f_u(Q)]^2 \times\frac{C(d_f-1)\Gamma(d_f-1)\xi^{d_f}}{(1+Q^2\xi^2)^{d_f/2}}\frac{(1+Q^2\xi^2)^{1/2}}{Q\xi} \times\frac{\sin[(d_f-1)\arctan(Q\xi)]}{d_f-1} \tag{2}$$

and

$$I_{\mathrm{self}}(Q)=\langle f_1(Q)\rangle-\langle f_u^2(Q)\rangle +x_px_w[\langle f_u(Q)\rangle\delta-\Delta f_u(Q)]^2+\langle I_{\mathrm{inc}}/4\pi\rangle, \tag{3}$$

where $x_w=(1-x_p)$, $\langle f_u(Q)\rangle$ is an averaged intermolecular form factor, δ a dilatation factor, C a constant, d_f a fractal dimension, ξ a persistence length for fractal correlations, $\Gamma(x)$ a gamma function, $\langle f_1(Q)\rangle$ an averaged intramolecular scattering intensity, and $\langle I_{\mathrm{inc}}\rangle$ an averaged incoherent scattering cross section. The $I_{\mathrm{self}}(Q)$ depends only on the intramolecular structure of individual molecules. The existence of salt was ignored in the analysis for simplicity because of the smallness of the amount.

C. Large-scale reverse Monte Carlo analysis

As the details of the large-scale RMC analysis have been reported in a previous paper,[4] a brief explanation is given here. Two structural units were introduced to perform the RMC analysis: One was a p unit which was composed of a single 1-propanol molecule and another was a w unit which was composed of four water molecules so that both had a similar volume of about 120 Å.[3] The equal volume of both units is essential in the present RMC analysis. A large number of the p units and the w units were distributed on a simple cubic lattice of a lattice constant a_0, 4.9 Å$(=120^{1/3}$ Å) in a cubic box of a size L with periodic boundary conditions. The size L was chosen to be about 300 Å, which was required by the SANS results, so that the number of the units in the box was about 2.5×10^5 in a typical case. These units were initially distributed randomly on the simple cubic lattice with a maximum fluctuation of $\pm0.3a_0$ around each lattice point. Then one of the p units and one of the w units were chosen randomly and they were interchanged. This procedure, that is, the random choice of two unlike units and the subsequent interchange of them, was repeated until the experimental SANS profile was reproduced by means of the

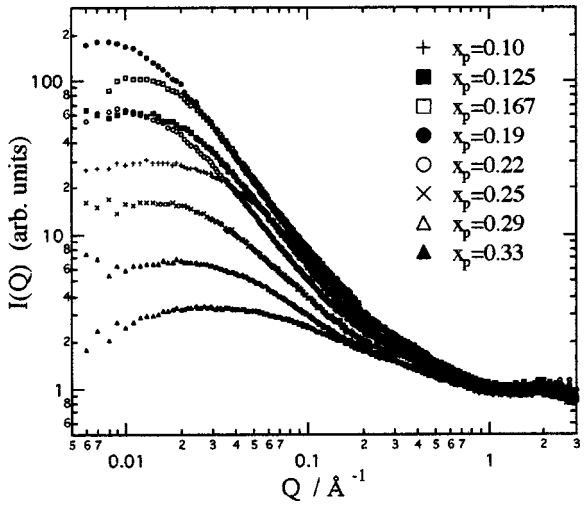

FIG. 1. SANS intensities measured for 1-propanol aqueous solutions at 25 °C. All curves are scaled at high Q.

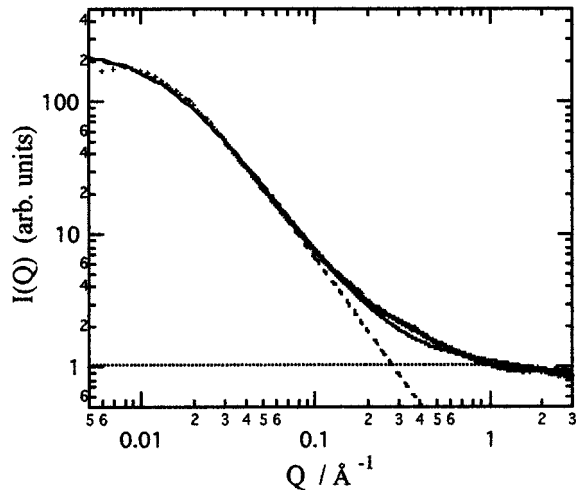

FIG. 2. Comparison of experimental SANS intensity (marks) and that fitted by fractal model (solid line) for 1-propanol aqueous solution of $x_p=0.19$. Broken line is fractal term [Eq. (2)] and dotted line is self-term [Eq. (3)].

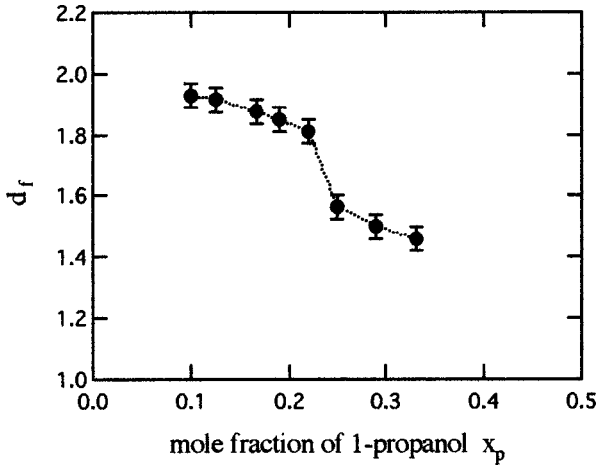

FIG. 3. Fractal dimension d_f obtained by fitting of $I(Q)$ to fractal model.

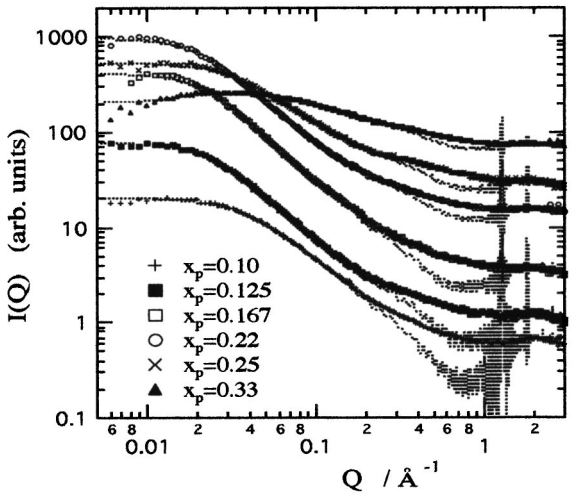

FIG. 4. Comparison of experimental SANS intensity $I(Q)$'s (marks) and those obtained by RMC modeling (dotted lines). Each $I(Q)$ curve is shifted in vertical scale for clarity.

standard reverse Monte Carlo technique.[9] The existence of salt was ignored in the RMC analysis for simplicity because of the smallness of the amount.

III. RESULTS

Figure 1 compares the experimental SANS intensities $I(Q)$ measured for the solutions at 25 °C. Equation (1) was fitted to each $I(Q)$ curve to obtain the fractal dimension of each solution. A typical example of the fit is shown in Fig. 2 for the solution of $x_p = 0.19$. The value of the fractal dimension d_f obtained for each solution is shown in Fig. 3 and listed in Table II. It is about 1.8–1.9 for the water-rich solutions, while it decreases to about 1.5 for the propanol-rich solutions. A clear change in the slope of the plot is recognized around $x_p = 0.22-0.25$. Some change appears to occur in the mesoscale structure of the solution around this composition.

In order to see what happens in the solution we performed the large-scale RMC analysis for the solutions studied except for the two solutions of $x_p = 0.19$ and 0.29. Figure 4 compares the experimental $I(Q)$'s and the RMC results. The fit for each solution is reasonably good over a wide range of Q except for the high Q region where some discrepancy is seen. It should be, however, noted that the vertical scale of Fig. 4 is a logarithmic scale so that the discrepancy at high Q is not significant: In fact if we plot these curves on a linear scale we cannot distinguish the RMC results from the experimental data. Therefore we think that the discrepancy at high Q is not significant as far as the mesoscale structure is concerned. Figure 5 shows the distributions of the p units and the w units in a thin layer of $2a_0$ thick obtained by the RMC analysis for the three solutions of $x_p = 0.125$ (upper graphs), 0.22 (middle graphs), and 0.33 (lower graphs). Concentration fluctuation, or clustering of the p units or the w units, is clearly seen in each plot. The gray symbols indicate the units located on the interface between unlike clusters, while the dark ones are those inside clusters. These are discussed later in detail.

The structure obtained by RMC modeling is analyzed in terms of percolation.[10] We define a cluster as follows: If the distance r between any two like units satisfies the relation $r \leqslant \sqrt{2}a_0$, the two units belong to the same cluster. The size of the cluster is defined as the number of units n of which the cluster is composed. Figures 6(a) and 6(b) show the distribution of the cluster size $\phi(n)$ for the p clusters (the clusters composed of the p units) and the w clusters (the clusters composed of the w units) for the solutions studied. As clearly seen in Figs. 6(a) and 6(b) each $\phi(n)$ is expressed by a

TABLE II. Fractal dimension d_f and persistence length of fractal correlations ξ in Eq. (2) determined by small angle neutron scattering. Mass fractal dimension d_M in Eq. (5) and exponent τ of cluster-size distribution in Eq. (4) determined by RMC modeling for p clusters and w clusters.

			p clusters		w clusters	
x_p	d_f	ξ (Å)	τ	d_M	τ	d_M
0.10	1.93±0.04	21	1.35±0.05	2.28±0.03	1.20±0.05	2.43±0.03
0.125	1.91±0.04	41	1.38±0.05	2.30±0.03	1.20±0.05	2.44±0.03
0.167	1.88±0.04	50	1.42±0.05	2.42±0.03	1.16±0.05	2.44±0.03
0.19	1.85±0.04	74	⋯	⋯	⋯	⋯
0.22	1.81±0.04	51	1.47±0.05	2.48±0.03	1.13±0.05	2.31±0.03
0.25	1.57±0.04	35	1.48±0.05	2.66±0.03	1.11±0.05	2.33±0.03
0.29	1.50±0.04	20	⋯	⋯	⋯	⋯
0.33	1.46±0.04	11	1.50±0.05	2.66±0.03	1.05±0.05	2.14±0.03

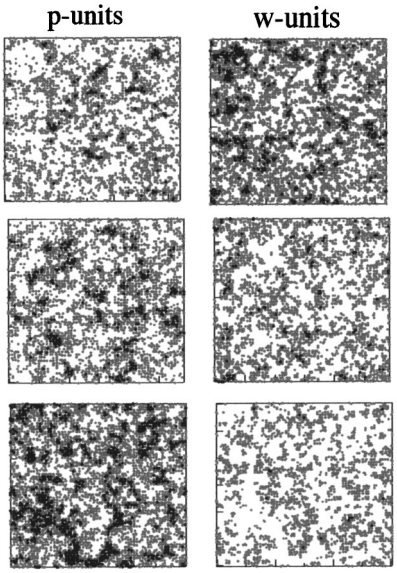

FIG. 5. Distribution of *p* units (left graphs) and *w* units (right graphs) in $2a_0$ thick layer along *z* axis obtained from RMC analysis for 1-propanol aqueous solutions of $x_p=0.125$ (upper graphs), 0.22 (middle graphs), and 0.33 (lower graphs). Gray symbols denote units located on interface between clusters, and dark ones those inside clusters. Lengths of side of box are 326 (upper), 296 (middle), and 306 Å (lower), respectively.

simple power law[10] with an exponential decay factor given by

$$\phi(n)\propto n^{-\tau}\exp(-n/n_0), \tag{4}$$

where n_0 is a decay constant. The values of exponent τ estimated for the *p* clusters and *w* clusters are listed in Table II. The value for the *p* clusters increases from 1.35 to 1.50 with increasing x_p, while that for the *w* clusters decreases from 1.20 to 1.05 with increasing x_p.

The spatial distribution of the units in a single cluster is examined in terms of a mass fractal,[11] for which the number of units $M(r)$ included in a sphere of radius *r* drawn in a cluster is scaled to *r* as given by Eq. (5),

$$M(r)\propto r^{d_M}, \tag{5}$$

where d_M is a dimension of mass fractal. In the present analysis the $M(r)$ is evaluated as follows: For a single cluster we draw many spheres of radius *r*, each of which has its center on one of the units in the cluster, and then we evaluate the $M(r)$ as the number of units inside the sphere averaged over all the spheres. Figure 7 shows some examples of the $M(r)$ curves of *p* clusters and *w* clusters obtained for the solutions of $x_p=0.167$ (a) and $x_p=0.33$ (b). As clearly seen from Figs. 7(a) and 7(b), the $M(r)$ satisfies the characteristics of a mass fractal given by Eq. (5) over about one decade. The value of d_M estimated by fitting Eq. (5) to the data is listed in Table II and plotted in Fig. 9(a) as a function of x_p. The values are about 2.3–2.5 for both the clusters in the water-rich solution, while they deviate much from these values in the propanol-rich solution. The value of 2.5 is close to the value of d_M obtained for diffusion-limited aggregation.[12]

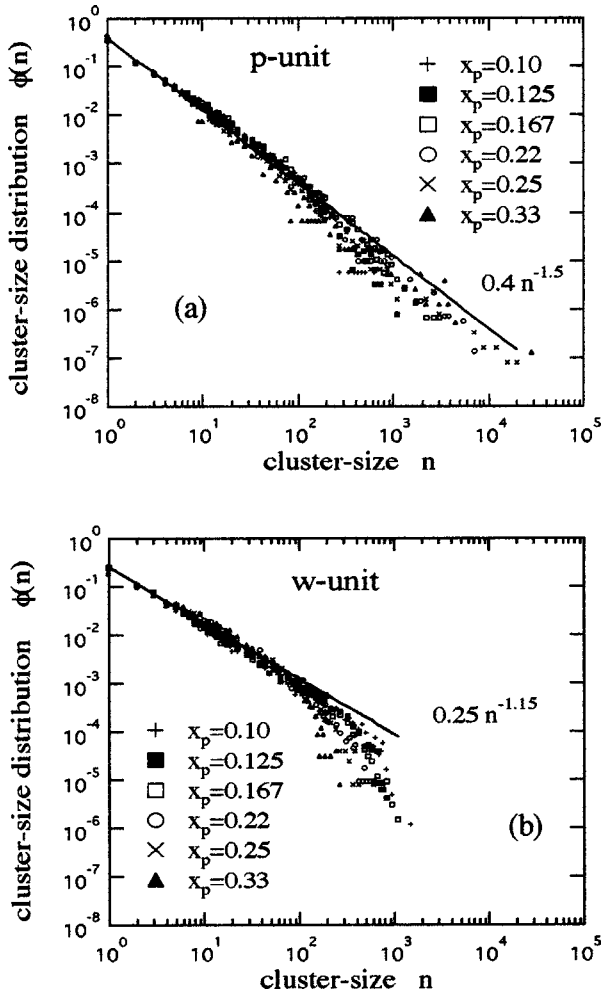

FIG. 6. Cluster-size distributions for *p* clusters (a) and *w* clusters (b) calculated from RMC results.

IV. DISCUSSION

A percolation theory[13] of polydisperse mass fractals predicts a relation among the three exponents d_f, d_M, and τ,

$$d_f=d_M(2-\tau). \tag{6}$$

This relation was obtained[13] by averaging a two-particle correlation function $g_n(r)$ for a single cluster of mass fractal of size *n* with a weight of cluster-size distribution $\phi(n)$. A slightly different expression $d_f=d_M(3-\tau)$ was proposed for this relation in Ref. 14, where it was calculated in *Q* space by averaging the scattering intensity $I_n(Q)$ from a single cluster of size *n* weighted with the $\phi(n)$. There is a contradiction between the two expressions. It is shown, however, that if one uses the exact scattering function of fractal for $I_n(Q)$, one gets the same result as Eq. (6) (see the Appendix). We calculate the right-hand side of Eq. (6) by substituting the experimental values of d_M and τ listed in Table II, and compare the result with the experimental value of d_f of the left-hand side of Eq. (6) in Fig. 8. The values calculated from Eq. (6) for the *w* clusters are close to the experimental values of d_f at the water-rich region, on the other hand those for the *p* clusters are close to the experimental values of d_f at the propanol-rich region. This fact implies that by the diffraction experiment we see predominantly the fractal dimension d_f of

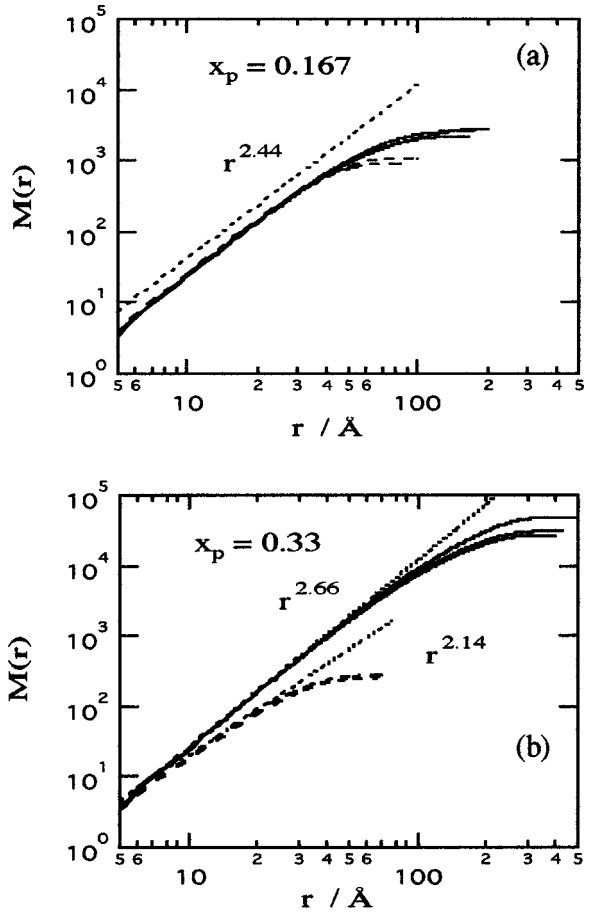

FIG. 7. $M(r)$ curves for p clusters (solid lines) and w clusters (broken lines) plotted as a function of r for 1-propanol aqueous solutions of $x_p=0.167$ (a) and 0.33 (b). $M(r)$'s shown are calculated for three larger clusters sampled in order of their size in each solution. These three $M(r)$ curves for p clusters (or w clusters) are very similar to each other in each solution. This result indicates that the present sampling of clusters is good enough to evaluate characteristics of clusters.

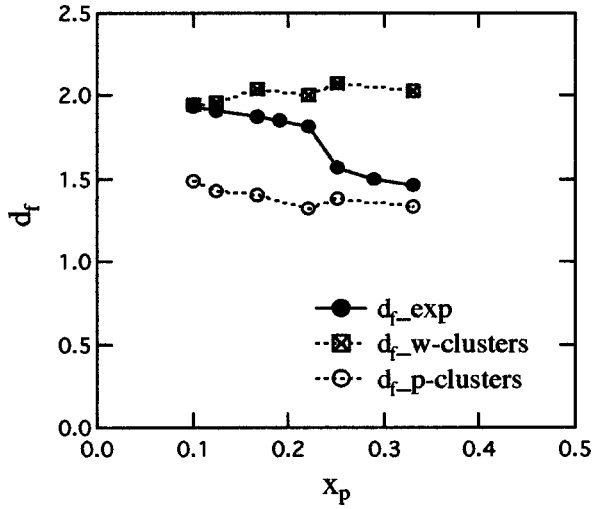

FIG. 8. Comparison of values of $d_M(2-\tau)$ calculated from Eq. (6) for p clusters (open circles) and w clusters (squares with cross), with experimental d_f (solid circles).

the w clusters for the water-rich solution while that of the p clusters for the propanol-rich solution. This is reasonable because of the following consideration: As the SANS intensity from polydisperse clusters is roughly proportional to $\int n^2\phi(n)dn$ times the total number of clusters, a simple calculation by substituting $\phi(n)$ given in Fig. 6(a) or 6(b) for that in the above equation shows that the intensity from the w clusters is estimated to be one order of magnitude larger than that from the p clusters in the solution of $x_p=0.1$. On the contrary, the intensity from the p clusters is two orders of magnitude larger that that from the w clusters in the solution of $x_p=0.33$, and a crossover occurs around $x_p=0.2$. Therefore we can conclude that the clear change in d_f around x_p of 0.22–0.25 can be attributed to the crossover between the water-rich regime and the propanol-rich regime.

The percolation theory[13] gave other relations between critical exponents and fractal dimensionalities: The Fisher exponent[15] η was given by $\eta=2-d_M(2-\tau)$, and a ratio of γ/ν (Ref. 15) was given by $\gamma/\nu=d_M(2-\tau)$. We calculate the values of the right-hand side of these relations by inserting the experimental values of d_M and τ listed in Table II for the p clusters and the w clusters. The results are shown in Figs. 9(c) and 9(d) as a function of x_p. In Figs. 9(a) and 9(b) the values of d_M and τ are also plotted. It is clearly seen from these plots that the values calculated for both clusters are very different from each other. The theoretical values of d_M, τ, η, and γ/ν obtained on various percolation models were reviewed in Ref. 16. Because these values are somewhat scattered, we plot the scattered range of these values by a pair of horizontal dotted lines in each of Figs. 9(a)–9(d). It is clearly seen from these figures that the values for the w clusters are qualitatively in good agreement with the theoretical predictions. This suggests that the w clusters play an essential role in the reentrant phase-separation of the current solution. However, we do not know the reason why only the water clusters agree with the theoretical predictions. We do not think that the present result is an artifact due to the assumptions used in the present RMC analysis such as (1) the simple cubic lattice arrangement of the units and (2) the coarsening of the structure units (or a grouping of four water molecules), because (1) Meakin[12] showed that the simple cubic lattice simulation and the nonlattice simulation gave the same value of Hausdorff (fractal) dimensionality and (2) our previous RMC analysis[4] showed that the small unit of a single water molecule and the coarse unit of a group of four water molecules gave the same value of the fractal dimension in the solution of $x_p=0.167$.

The interface between the clusters is analyzed in terms of percolation as well. The interface is defined as follows: If the distance r between any two unlike units satisfies the relation $r\leqslant\sqrt{2}a_0$, the two units are located on interface. The gray units shown in Fig. 5 are those determined in this way. Figure 10 shows the ratio of the p units located on the interface to all the p units, and also that of the w units. The ratios for both units are larger than 0.8 for all the compositions studied. This implies that most molecules are located on the interface as far as the above definition is accepted. By a simple extrapolation of the ratio of the p units to lower x_p, it crosses 1.0 at x_p near 0.05. This expectation suggests that all the p units are located on the interface or almost isolated

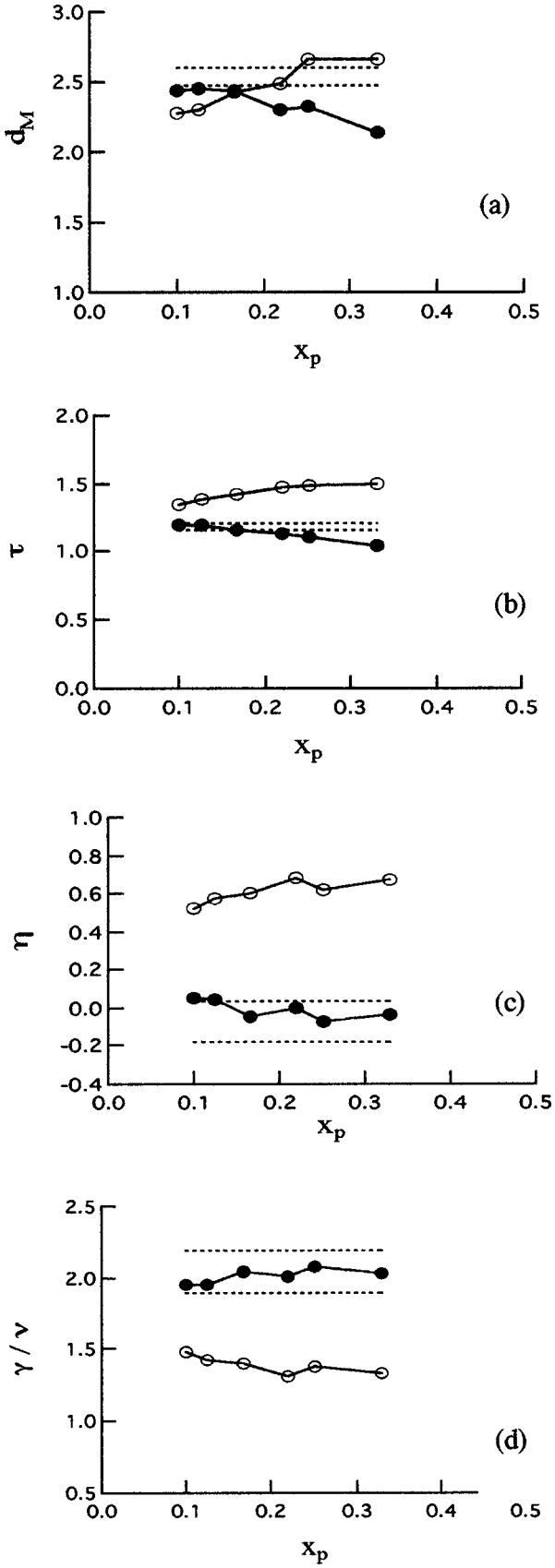

FIG. 9. Comparison of some exponents obtained from RMC results for *p* clusters (open circles) and *w* clusters (solid circles): Mass-fractal dimension d_M (a), exponent for size distribution τ (b), Fisher exponent η (c), and ratio γ/ν (d). Theoretical values predicted by various percolation models (Ref. 16) are distributed between two dotted lines in each graph.

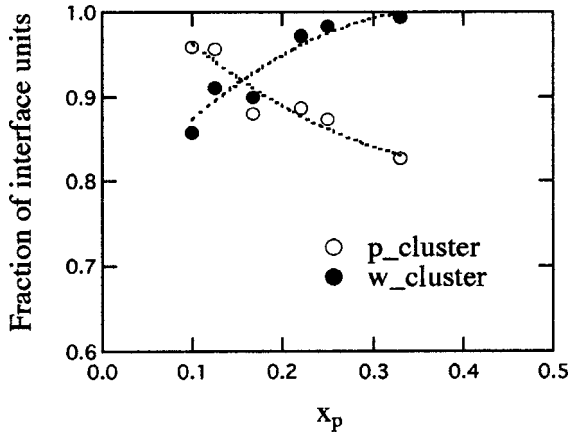

FIG. 10. Fractions of interface units for *p* clusters and *w* clusters analyzed from RMC results. Dotted lines are guides for eyes.

below this composition. This composition of 0.05 is close to the transition region from the mixing scheme I (where the isolated propanol molecules are dominant) to the scheme II (where cluster formation is dominant) proposed by Koga[17] from the thermodynamic point of view.

The thickness of the *w* clusters is evaluated in the similar way as before,[4] except for the way of sampling the interface units: In the previous paper[4] the thickness of the water layer was evaluated for particular interface *p* units selected in a rather complicated way, while in the present analysis it is evaluated for all the interface *p* units defined above. The thickness distribution of the water layers calculated for each solution studied here is shown in Fig. 11. Because the present result for the solution of $x_p = 0.167$ is essentially the same as the previous result for the same solution,[4] the thickness distribution shown in Fig. 11 is insensible to the details of the definition of interface and the way of sampling the interface units. Therefore we think that the results shown in Fig. 11 are reliable. As clearly seen in Fig. 11 the center of the distribution curve is located at about 10 Å or less for all the solutions studied. Based on the previous results[4] on the thickness distribution for the salt-free solution and that for the salt-added solution, the thickness distribution shown in

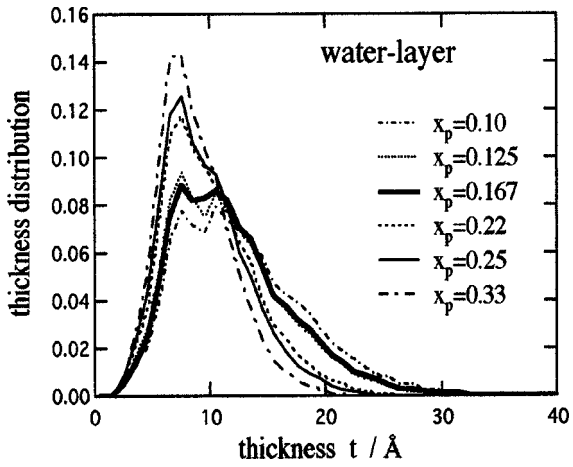

FIG. 11. Thickness distribution of water layers analyzed from RMC results. Calculation was done by using search angle (Ref. 4) of ϕ=20°.

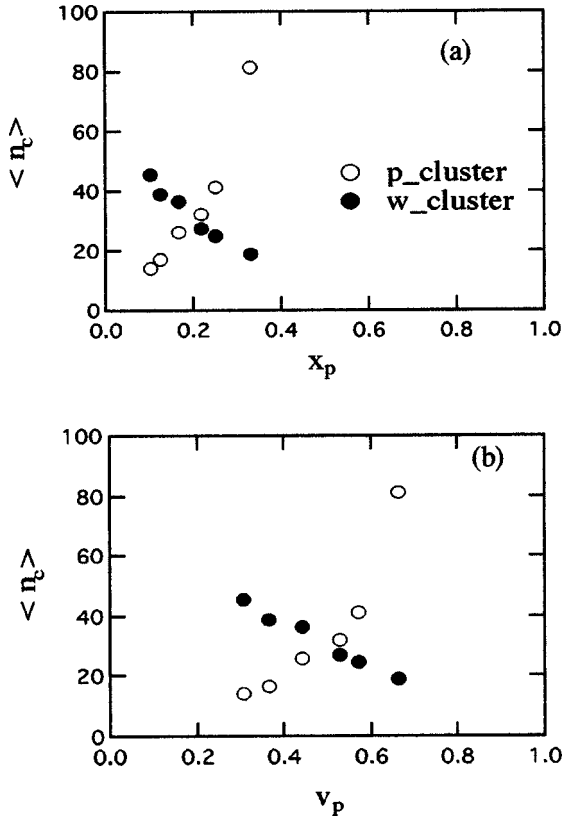

FIG. 12. Mean cluster-size $\langle n_c \rangle$ evaluated from RMC results plotted for mole fraction x_p (a) and volume fraction v_p (b) of 1-propanol.

Fig. 11 may shift toward smaller value if the salt is removed from the solution. Therefore it is strongly suggested that the thin water layer of 10 Å thick or less is stable in the current solution irrespective of the propanol content studied. The quasielastic neutron scattering results on the current solution[18] showed that the motion of water molecules was suppressed by a factor of 2 compared to that for pure water even for the dilute solution of $x_p=0.075$ and the degree of suppression did not change much for more concentrated solution of $x_p=0.167$. This result indicates that the dynamical states of the solvent water for both compositions are similar. This fact may also support the formation of the stable thin water-layers irrespective of the propanol content from a dynamical point of view.

Figures 12(a) and 12(b) show the mean cluster size $\langle n_c \rangle$ as a function of the mole fraction x_p and the volume fraction v_p of 1-propanol, respectively. The x_p dependence of $\langle n_c \rangle$, or v_p dependence of $\langle n_c \rangle$, is different for the *p* clusters and the *w* clusters: The $\langle n_c \rangle$ for the *p*-clusters increases steeply with increasing x_p or v_p and seems to be infinity near $x_p=0.4$ (or $v_p=0.7$–0.8) which is far below $x_p=1.0$ (or $v_p=1.0$) of the pure state, while for the *w* clusters it depends rather gradually on x_p or v_p compared to that of the *p* clusters and seems to be finite even close to the pure state. As a whole the size of the *w* clusters is small in comparison with that of the *p* clusters. This result is already shown in a different way in Figs. 6(a) and 6(b): The maximum size of the *w* clusters is one or two orders of magnitude smaller than that of the *p* clusters. The characteristics in the intermolecular interaction for both molecules, especially the hydrogen bonding between the water molecules, may play an important role in these differences.

V. CONCLUSION

The neutron small angle scattering data on the 1-propanol aqueous solution show that the mesoscale structure of the solution is characterized by a fractal with the fractal dimension d_f of about 1.8–1.9 for the water-rich solution and about 1.5 for the propanol-rich solution. The large-scale reverse Monte Carlo analysis performed for the solution reveals that the water molecules and the propanol molecules form clusters, respectively: The structure of both clusters is characterized by a mass fractal with the dimension d_M of about 2.3–2.5 for water-rich solution, and the cluster-size distribution is characterized by the simple power law with the exponent τ of about 1.35–1.5 for the *p* clusters and 1.05–1.2 for the *w* clusters. Both values of d_M and τ depend systematically on the composition x_p. A theoretical relation $d_f=d_M(2-\tau)$ predicted for the polydisperse mass fractals holds well in the current solution. The characteristic change in d_f from 1.8–1.9 to 1.5 is attributed to the crossover between the water-rich regime and the propanol-rich regime. The critical exponents estimated for the *w* clusters are qualitatively in good agreement with the theoretical predictions, while those for the *p* clusters are not. These facts suggest that the *w* clusters play an essential role in the reentrant phase separation of the current solution. Most of the water molecules and the propanol molecules are located on the interface between the clusters. It is suggested that the solvent water forms the thin layers of about 10 Å thick or less irrespective of the propanol content studied. The size of the *w* clusters is small in comparison with that of the *p* clusters.

It is very interesting to examine whether the above findings, especially the mass fractal clustering of water molecules and the formation of stable thin water layer, are common characteristics of the solvent water in solutions of this kind, or they are peculiar to the current solution. More extensive work on the aqueous solution, including biology-related solution, is needed to clarify these aspects.

APPENDIX: A RELATION AMONG d_f, d_M, AND τ

A pair correlation function $g_n(r)$ of a cluster of mass fractal of finite size with a fractal dimension d_M and a persistence length of fractal correlations ξ is given by[8]

$$g_n(r) \propto r^{d_M-d} \exp(-r/\xi). \tag{A1}$$

If this cluster is composed of *n* particles, it is plausible to assume that *n* is approximately related to ξ as

$$n \propto \xi^{d_M}. \tag{A2}$$

The scattering function $I_n(Q)$ of the cluster is given by the Fourier transform of Eq. (A1),[8]

$$I_n(Q) \propto \xi^{d_M} F(Q\xi, d_M), \tag{A3}$$

where

$$F(Q\xi,d_M)=\frac{C(d_M-1)\Gamma(d_M-1)}{(1+Q^2\xi^2)^{d_M/2}}\frac{(1+Q^2\xi^2)^{1/2}}{Q\xi}\times\frac{\sin[(d_M-1)\arctan(Q\xi)]}{d_M-1}. \quad \text{(A4)}$$

Then the scattering intensity $I(Q)$ from polydisperse mass fractals of size distribution $\phi(n)$ is given by[14]

$$I(Q)\propto\int_0^\infty I_n(Q)\phi(n)dn \propto\int_0^\infty \xi^{d_M}F(Q\xi,d_M)n^{-\tau}\exp(-n/n_0)dn. \quad \text{(A5)}$$

Here we ignore the intercorrelations among fractal objects. By using Eq. (A2) and changing the variable $Q\xi=x$, we have

$$I(Q)\propto Q^{-d_M(2-\tau)}\int_0^\infty x^{d_M(2-\tau)-1}F(x,d_M)\times\exp(-(x/x_0)^{d_M})dx, \quad \text{(A6)}$$

where $x_0=Q\xi_0=Qn_0^{1/d_M}$. If ξ_0 is large enough, the integral of the above equation is independent of Q except for very small Q, $Q\xi_0\ll 1$. Then $I(Q)$ is proportional to $Q^{-d_M(2-\tau)}$, so that we have the same relation as Eq. (6) in Q space,

$$d_f=d_M(2-\tau). \quad \text{(A7)}$$

At very small Q, $Q\xi_0\ll 1$, it is shown that $I(Q)$ is independent of Q, i.e., $I(Q)\propto\xi_0^{d_M(2-\tau)}\propto\xi_0^{d_f}$, as expected for a finite system.

[1] T. Narayanan and A. Kumar, Phys. Rep. **249**, 135 (1994).
[2] G. M. Schneider, Ber. Bunsenges. Phys. Chem. **76**, 325 (1972).
[3] K. Yoshida, M. Misawa, K. Maruyama, M. Imai, and M. Furusaka, J. Chem. Phys. **113**, 2343 (2000).
[4] M. Misawa, J. Chem. Phys. **116**, 8463 (2002).
[5] T. Otomo, M. Furusaka, S. Satoh, S. Itoh, T. Adachi, S. Shimizu, and M. Takeda, J. Phys. Chem. Solids **60**, 1579 (1999).
[6] M. Misawa, I. Dairoku, A. Honma, Y. Yamada, T. Sato, K. Maruyama, K. Mori, S. Suzuki, and T. Otomo, J. Neutron Res. (in press).
[7] B. B. Mandelbrot, *The Fractal Geometry of Nature* (Freeman, New York, 1983).
[8] T. Freltoft, J. K. Kjems, and S. K. Sinha, Phys. Rev. B **33**, 269 (1986).
[9] R. L. McGreevy and L. Pusztai, Mol. Simul. **1**, 359 (1988).
[10] D. Stauffer and A. Aharony, *Introduction to Percolation Theory* (Taylor & Francis, London, 1998).
[11] J. F. Gouyet, *Physics and Fractal Structures* (Masson, Paris, 1996).
[12] P. Meakin, Phys. Rev. A **27**, 1495 (1983).
[13] H. Tasaki, J. Stat. Phys. **49**, 841 (1987); H. Tasaki, in *Fractal Science*, edited by H. Takayasu (Asakura, Tokyo, 1987), Chap. 4, in Japanese.
[14] J. E. Martin, J. Appl. Crystallogr. **19**, 25 (1986).
[15] H. E. Stanley, *Introduction to Phase Transitions and Critical Phenomena* (Oxford University Press, Oxford, 1971).
[16] J. Adler, Y. Meir, A. Aharony, and A. B. Harris, Phys. Rev. B **41**, 9183 (1990).
[17] S. H. Tanaka, H. I. Yoshihara, A. W.-C. Ho, F. W. Lau, P. Westh, and Y. Koga, Can. J. Chem. **74**, 713 (1996).
[18] M. Misawa, K. Yoshida, K. Maruyama, H. Munemura, and Y. Hosokawa, J. Phys. Chem. Solids **60**, 1301 (1999).